GLOBAL DISTRIBUTION AND CHARACTERISTICS OF DOMICAL CRATERS ON THE MOON

Nandita Kumari[1,2], Harish Nandal[2], Indhu Varatharajan[3], Ritu Anilkumar[4], Kanmani Shanmugapriya[1] and Vijayan S[2]
[1]Institute of Remote Sensing, Anna University, Chennai (Email: nandita.ceg@gmail.com), [2]Physical Research Laboratory, PSDN, Ahmedabad, [3]Institute of Planetary Research, DLR, Berlin, [4]North-Eastern Space Application Centre, Meghalaya

Introduction: On Moon, there are reports of small to large scale domes which are the result of extrusive volcanism [1,2]. Such domes are present within mare regions and predominantly associated to same [1]. However, dome like structures or convex up floors have also been reported inside some craters with fractures on it, under the class of Floor Fracture Craters(FFCs)[3,4]. Domical craters are a class of lunar craters defined by their distinctly convex-up uplifted, often reverted bowl like floors. The dome inside these craters make them an ideal candidate to study the evolution and influence of underlying stalled magma in a constrained condition which are likely present over different parts of moon. Moreover, craters with domical floor uplift will provide significant information about the intrusions that occurred into the lunar crust [3,4]. In this study, we have analyzed the formation mechanisms for the fractures in these FFCs which were initially proposed to be due to maximum bending during the floor uplift due to sill intrusion [4] and the dome formation. Thus, the purpose of this study is to provide a global catalog of the locations, classes and topographic, morphologic and mineralogic characteristics of the lunar domical craters. We have also constrained the formation epoch of these craters.

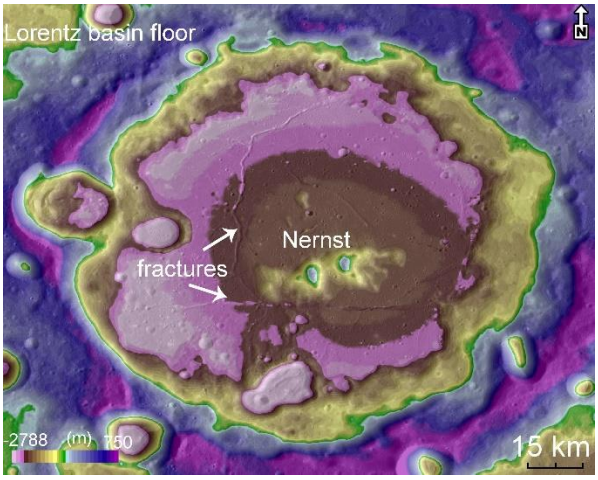

Fig 1. LRO-LOLA color coded image of Nernst crater with convex-up floor; located inside the Lorentz basin

Methods: We used Lunar Reconnaissance Orbiter (LRO) Lunar Orbiter Laser Altimeter (LOLA), Lunar Reconnaissance Orbiter Camera (LROC), Chandrayaan-1(Moon Mineralogy Mapper M^3) and GRAIL crustal thickness map in our study. Using Jowiak [3] as an initial reference, the identified FFCs were examined to distinguish those with convex-up uplift spread across the entire floor (Fig. 1). Consequently, we undertook a global survey of the LROC Wide-Angle Camera (WAC) data overlaid on LOLA-SELENE Merger data to identify those domical craters and identified 16 such craters (Fig. 2).

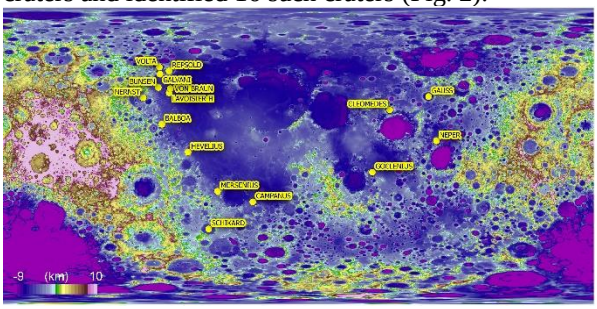

Fig 2. LRO-LOLA global color-coded image with the distribution of domical craters.

We used the association to basin as described in Jowiak [4] as the base for classification. The domical craters have been therefore classified into two categories: (1) Associated domical craters: these craters are located within or on the outer rims of the basin (2) Isolated domical craters: these craters are not located within or on the rim of any basin. The outer rims of the lunar basin have been taken from Neumann [5]. Seven craters were classified as associated domical craters and nine craters were classified as isolated domical craters. The diameter of these craters varied from ~30km to ~200km.

Result and Discussion: We observed 9 craters with fractures extending beyond the crater rims (Fig. 3) and 6 craters with fractures within them. This suggest that the extent of these fractures differs with the local geological setting. Crater Schickard does not display any fractures on its floor. Among the craters overlaid with fractures extending beyond their rims, 3 were associated domical craters and 6 were isolated domical craters. In addition, we also observed all the associated domical craters to host graben concentric to their adjoining basin. Using GRAIL crustal thickness maps, we found the crustal thickness to be varying from ~20 km to ~46 km within these craters. The crustal thickness for associated domical craters with basin varied from

~20 km to ~46 km and the crustal thickness for isolated domical craters varied from ~30 km to ~42 km.

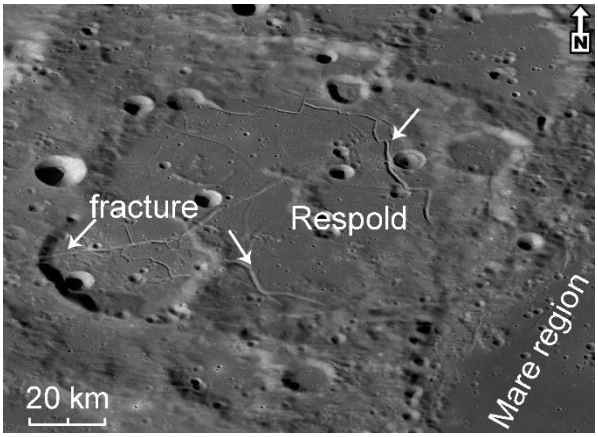

Fig 3. LRO-WAC image of Repsold crater (isolated domical crater) with fractures extending beyond the crater rim.

We used topography data to identify the variation in dome height among these craters. The dome height within these craters varied from ~180 m to ~840 m. Within, associated domical craters, it varied from ~180m to ~840 m and within isolated craters it varied from ~300 m to ~780 m. We also calculated the height of the central peak from dome maxima, however, not all craters displayed central peaks within their floors. 4 craters lacked central peaks in which none were associated domical craters. The central peak height varied from ~180 m to ~2280 m. The associated domical craters displayed their central peak heights varying from ~180 m to ~2280 m while the isolated craters displayed central peaks heights varying from ~240 m to ~1020 m.

From M^3 mineralogical analysis we identified presence of crystalline plagioclase (PAN), spinel, pyroclastic deposits(Glass) and pyroxene-ortho and clino (Fig. 4). The crystalline plagioclase was observed on the central peak of four craters (Nernst, Neper, Cleomedes and Gauss). Among these, Gauss is an isolated domical crater while other three are associated domical crater. Spinel was observed only on the central peak of Neper-an associated domical crater. Pyroclastic deposits were observed on the crater floor of one associated domical crater (Goclenius) and an isolated domical crater (Gauss). These were observed in pits within these craters. Pyroxene was observed on thefloor of all the craters. In that, 6 craters displayed signatures of only orthopyroxene and 2 craters displayed signatures of only clinopyroxene, the remaining 8 craters hosted a mixture of both ortho and clinopyroxene. Thus 10 craters showed signature of clinopyroxene and among the 10 craters, 8 hosted pigeonite in dominance. It is to be noticed that Gauss and Goclenius also had pyroxene lithology which makes it difficult to differentiate pyroclastic deposits from them**.** The pyroclastic deposits were identified in these craters due to their association with dark-albedo annulus and their band centres which are after 1µm and near 2 µm [6]. The pyroxene signatures were observed on the floor, along the fractures, central peak and walls of the craters.

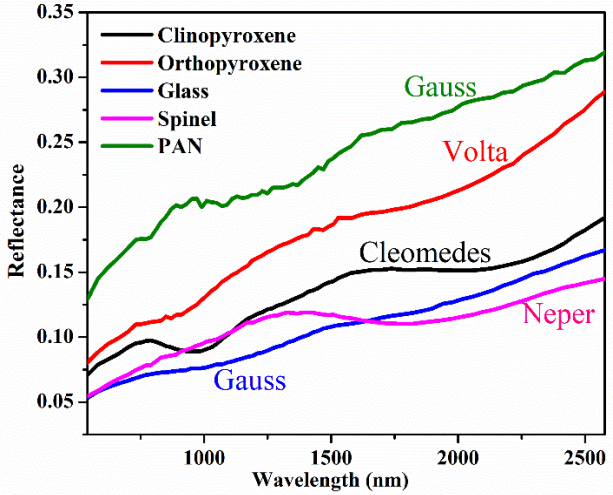

Fig 4. M^3 derived reflectance spectra from different domical craters suggestive of the diverse mineral presence

A detailed crater size frequency distribution was carried out over the crater domical floor to constrain their plausible formation epoch. We found the crater ages to be from Pre-Nectarian (~4.0 Ga) to Eratosthenian (~3.6 Ga) epoch. From our study we did not observe any domical craters post Eratosthenian.

Summary: The diverse mineralogy observed from the domical craters indicates towards the lateral heterogeneities in the lunar crust. Presence of fractures cutting through the rims of the craters indicates towards their real extent and it is not plausibly constrained within the crater. The domical craters within the basins suggest that the basins likely played a role in crustal thinning, this we interpret from the magma intrusion in highlands as observed in Nernst crater. The crater chronology constraints the formation of these craters to Eratosthenian epoch.

References: [1]James W. Head and Ann Gifford(1980), Earth Moon and Planets,235-258 [2]Ivanov.M et. al.(2015), *Icarus*,262-283, Vol. 273[3]Jozwiak L. M et. al.(2012), *JGR*, Vol 117, E11005 [4] Jozwiak L. M et. al.(2014), *Icarus*, 424-447, Vol. 248[5] Neumann G.A et.al(2015), *Science Advances, DOI: 10.1126/sciadv. 1500852* [6]Horgan, B et. al.(2014), *Icarus*, 132-154, Vol. 234